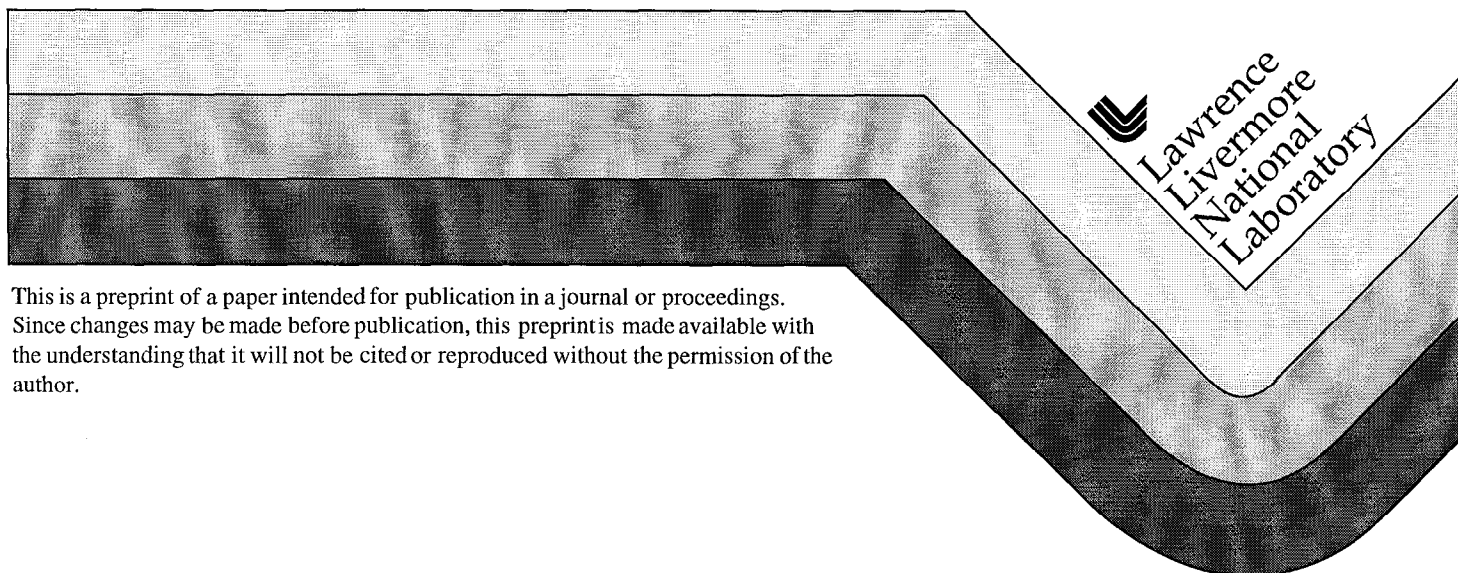


High-Power Reliable Operation of InGaAsP/InP Laser Bars at 1.73 μm

J. A. Skidmore
R. H. Page
B. L. Freitas
C. E. Reinhardt
E. J. Utterback
M. A. Emanuel

This paper was prepared for submittal to the
International Conference on Lasers '98
Tucson, Arizona
December 7-11, 1998

February 16, 1999



DISCLAIMER

This document was prepared as an account of work sponsored by an agency of the United States Government. Neither the United States Government nor the University of California nor any of their employees, makes any warranty, express or implied, or assumes any legal liability or responsibility for the accuracy, completeness, or usefulness of any information, apparatus, product, or process disclosed, or represents that its use would not infringe privately owned rights. Reference herein to any specific commercial product, process, or service by trade name, trademark, manufacturer, or otherwise, does not necessarily constitute or imply its endorsement, recommendation, or favoring by the United States Government or the University of California. The views and opinions of authors expressed herein do not necessarily state or reflect those of the United States Government or the University of California, and shall not be used for advertising or product endorsement purposes.

High-Power Reliable Operation of InGaAsP/InP Laser Bars at 1.73 μm

J. A. Skidmore, R. H. Page, B. L. Freitas, C. E. Reinhardt, E. J. Utterback, and M. A. Emanuel

University of California Lawrence Livermore National Laboratory

P.O. Box 808, Livermore, CA 94550

jskidmore@llnl.gov

ABSTRACT

InGaAsP/InP laser bars with an emission wavelength of 1.73 μm have been fabricated using compressively-strained multiple-quantum-well separate-confinement heterostructures. One-cm-wide, 0.7-fill-factor, diode bars are bonded onto Si microchannel heatsinks. A maximum cw power of 16 W was produced from a one-cm bar. Derated to 8W cw, the extrapolated lifetime is 10,000 hours of operation with a 20% degradation in output power. A 10-bar microlensed diode array with a one-square-cm aperture produced 200 W of peak power and was focused onto a Cr:ZnSe slab laser. Over 3 watts of pulsed power was generated at a wavelength of 2.5 μm .

had xx mw of average power

I. INTRODUCTION

Commercial diode-pumped solid-state lasers (DPSSLs) generally contain either Nd- or Yb-doped crystals that are pumped by AlInGaAs and InGaAsP-based lasers emitting in the 800–980 nm wavelength range. By comparison, diode pumping at longer wavelengths (i.e., 1.5–2.0 μm) in the InP-based material system is not nearly as mature, despite the need for such applications as medical lasers and remote sensing. For example, both Tm:Ho:YAG (1.6 μm pump)[1,2] and Ho:YAG (1.9 μm pump)[3,4] could benefit from long-wavelength pumping to avoid the large quantum-defect penalty (partially mitigated in Tm by “2-for-1” cross-relaxation ion-ion energy transfer) when pumping at the standard (~ 800 nm) wavelengths.[1] Of particular interest, is a Cr²⁺:ZnSe laser which is capable of being tuned from 2.1 to 2.8 μm . [5] This wide tunability could someday be exploited for laser surgery because the absorption depth of tissue (i.e., water) varies nearly three orders of magnitude over this wavelength range.[6,7] Tuning a fiber-delivered laser scalpel would provide a high degree of flexibility for the operator depending on the surgical technique desired. To achieve such flexibility of wavelength control is impractical using other laser systems, e.g., a combination of different-wavelength lasers would still suffer from wide gaps over the requisite tuning range.

As a dopant:crystal combination, $\text{Cr}^{2+}:\text{ZnSe}$ offers several potential advantages to other laser systems. First, it has a broad absorption band (350 nm FWHM) that peaks at $\sim 1.78 \mu\text{m}$, as shown in Fig. 1. The broad absorption band eliminates the need for accurate diode wavelength control. The relatively high absorption cross section also allows for lower required irradiance of the crystal for efficient lasing action. This is an important consideration, since the peak power of the InP-based diode lasers is generally lower by several times compared to the near-IR AlGaAs/InGaAsP diodes. Finally, laser diodes pumping at $1.78 \mu\text{m}$ produce a relatively low quantum defect with respect to the $2.5 \mu\text{m}$ laser emission which is important for minimizing waste heat.

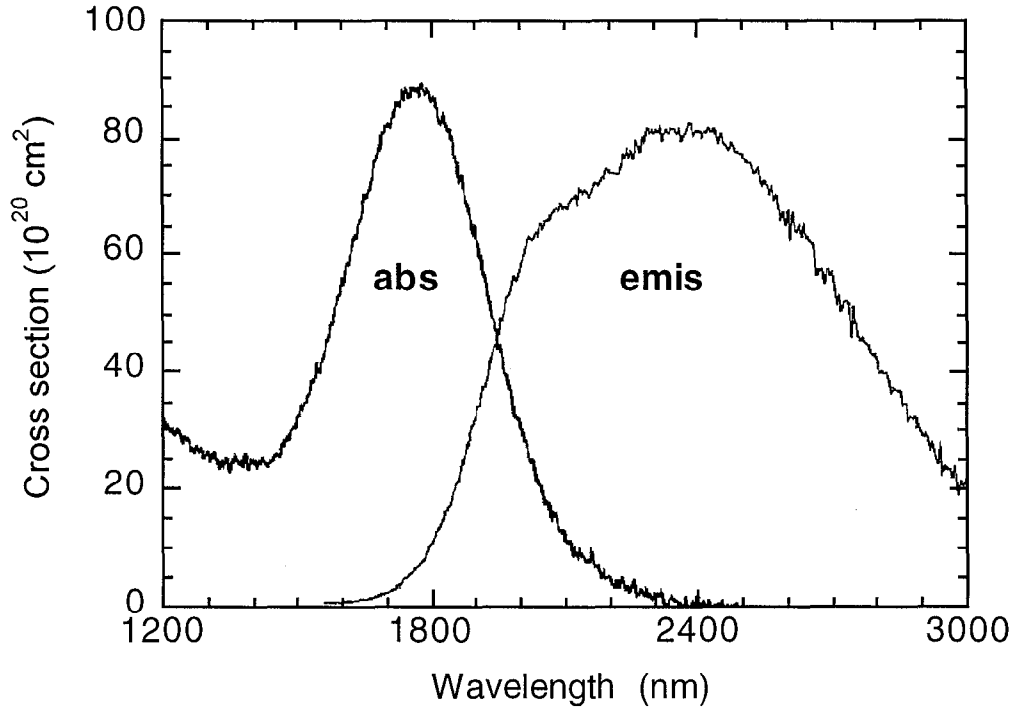


Fig.1. Absorption and emission cross section of the $\text{Cr}^{2+}:\text{ZnSe}$ laser. The broad absorption band eases the diode wavelength control, and the strong absorption allows for efficient lasing action at lower optical irradiance of the crystal. The wide emission cross section provides wide tunability ($2.1\text{--}2.8 \mu\text{m}$).

The InGaAsP/InP material system has been deployed reliably in long-haul ($1.55 \mu\text{m}$ wavelength) undersea telecommunication systems. However, only single, low-power emitters have shown efficient and reliable operation. Fabricating arrays is problematic because stacking emitters closely together introduces thermal cross talk which exacerbates Auger recombination, intervalence band absorption, and carrier leakage out of the quantum wells.[8,9] To compensate for the inherently poor thermal behavior of long-wavelength material, biaxial-compressively-strained quantum wells can reduce the transparency carrier density by reducing the in-plane heavy-hole mass. The use of multiple quantum wells (MQWs) can further reduce the carrier density per well [a crucial advantage, since Auger recombination increases dramatically with carrier density as it involves three-carrier interactions (i.e., $R_{\text{Auger}} \sim n^3$)].

It is equally important to utilize a heatsink with low thermal impedance for cw or high-average power operation. In this work, silicon microchannel coolers are used which possess a low normalized thermal impedance

(< 0.015 °C-cm²/W) in a scaleable two-dimensional architecture. The salient performance advantage of this heatsink comes from the incorporation of “microchannels” which lie just beneath the diode; their narrow width (20 μm) minimizes the stagnant boundary layer of water which contributes the bulk of the overall thermal impedance (the thermal impedance of water at room temperature is ~ 250 times greater than silicon). The design and characterization of the silicon microchannel heatsink have been given in detail previously.[10]

II. InGaAsP/InP LASER BARS

A schematic diagram of the MQW separate-confinement heterostructure (SCH) is shown in Fig. 2. The material was grown by metal organic chemical vapor deposition (MOCVD) on (100) n⁺ InP substrates.[11] Four 7-nm-thick compressively-strained In_{0.65}Ga_{0.35}As quantum wells were separated by 15 nm-thick InGaAsP ($\lambda_g = 1.25$ μm) barrier layers, all undoped. The InP cladding layers were both 1.6 μm thick and doped ~ 10¹⁸ cm⁻³. To reduce the series resistance, an InGaAsP ($\lambda_g = 1.25$ μm) barrier-reduction layer (50 nm thick) was grown between the p-cladding layer and the 100 nm-p⁺ In_{0.53}Ga_{0.47}As cap layer. Zn and S were used for the p- and n-type dopants, respectively. Except for the quantum wells, all material was grown lattice matched to the InP substrate.

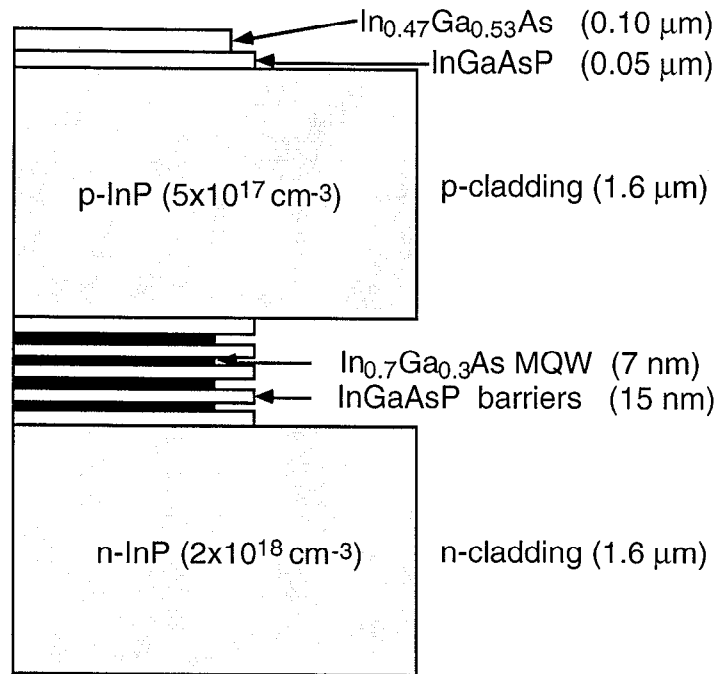


Fig.2. Schematic diagram of the compressively-strained InGaAs/InGaAsP quadruple-quantum-well, separate-confinement heterostructure (MQW-SCH) laser diode. The right-hand-side outline of the structure illustrates the energy of the conduction band.

The laser bars consist of 100 μm wide emitters spaced on 140 μm wide centers, producing a fill factor of 0.7. Each emitter was optically isolated from its neighbors by etching v-grooves between emitters. We found that a

mixture of $\text{HNO}_3\text{:HCl:H}_2\text{O}$ (2:1:1) produced a relatively non-selective etchant at room temperature so that the v-grooves would have smooth interfaces across different material boundaries. Plasma-enhanced chemical-vapor-deposition (PECVD)-grown SiO_2 is used for the electrical isolation as well as the etch mask. The p-side was metallized with Ti/Pt/Au, and afterwards, the wafer was thinned to $\sim 120\text{ }\mu\text{m}$ to facilitate cleaving. Ge/Au/Ni/Au was deposited onto the n-side and the contacts were then alloyed. After cleaving, the laser bars were facet coated using electron-beam evaporation. A $750\text{ }\mu\text{m}$ -long cavity was chosen to increase the slope efficiency for high-peak-power short-pulsed operation. Note that longer cavities would be more suitable for cw operation to dissipate the high thermal load. At an emission wavelength of $1.73\text{ }\mu\text{m}$, the low reflector (LR) had a reflectivity of $\sim 15\%$ using a single layer of Al_2O_3 , and the high reflector (HR) had a reflectivity of $\sim 85\%$ using an alternating quarter-wavelength stack of SiO_2/Si layers (three pairs total). Although additional layers would boost the backside reflectivity, it is avoided because these films may peel at these thicknesses. Once the laser bars were coated, they were indium-soldered, p-side down, to silicon microchannel heatsinks. Au wire bonds connected the n-side of the bar to the n-side contact of the package.

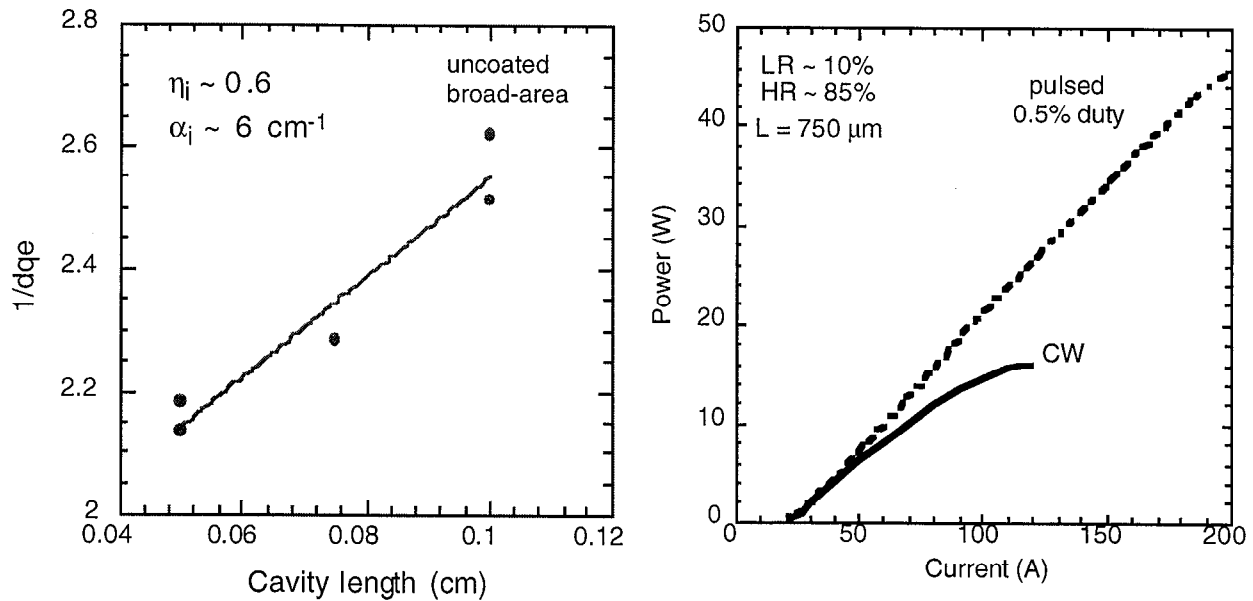


Fig.3. (a) Characterization of broad-area stripe lasers (uncoated) with different cavity lengths. (b) Light-current characteristics for a one-cm wide InGaAs laser bar with a 0.7 fill factor and a $750\text{ }\mu\text{m}$ cavity length. The device was operated under pulsed ($50\text{ }\mu\text{s}$ pulse widths at 100 Hz) and cw conditions. The coolant temperature was $11\text{ }^\circ\text{C}$.

The internal loss and the internal quantum efficiency were measured to be $\alpha_i = 6.0\text{ cm}^{-1}$ and $\eta_i = 0.60$, respectively (measuring characteristics of different length broad-area lasers), as shown in Fig. 3a. Laser bars fabricated from this same material were tested as shown in Fig. 3b. The light-current (L-I) characteristics are given for a $750\text{ }\mu\text{m}$ cavity length. Under pulsed operation ($50\text{ }\mu\text{s}$ at 10 Hz), the threshold current density (J_{th}) is roughly 460 A/cm^2 ($\sim 115\text{ A/cm}^2$ per quantum well) and the differential quantum efficiency (dqe) is 0.37 for our best laser

bar. As shown in the figure, 46 W was obtained under pulsed conditions (50 μ s at 100 Hz), which was supply limited at 200 A. At 85 A, the diode reaches its peak wall plug efficiency of 17%. When the laser bar was operated cw, a maximum output power of 16 W was attained at thermal roll over, which to our knowledge, is the highest value reported in this wavelength regime.[12] The peak wall plug efficiency of 14% occurs at 70 A, which illustrates the importance of extremely aggressive heatsinks for this application.

The output spectrum of the same laser bar package is shown in Fig. 4. At a cw drive current of 80 A (power level \sim 12 W), the peak emission intensity is centered at 1733 nm, and the full width at half maximum (FWHM) is 5.6 nm. Note that the wavelength is short by \sim 50 nm from the peak absorption of the ZnSe crystal. Because the absorption curve is broad (recall Fig. 1), and the diode performance degrades monotonically with longer wavelength, the lasing wavelength was designed comfortably short of the peak absorption of the crystal.

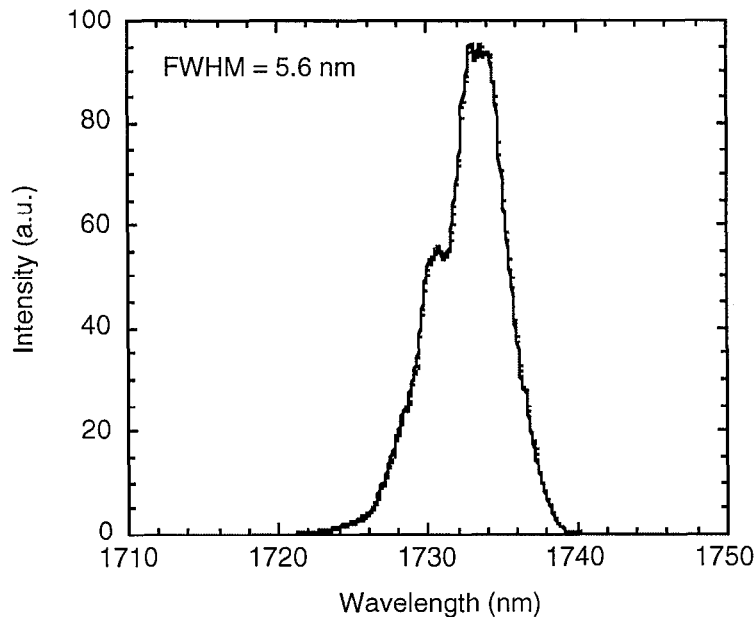


Fig.4. Emission spectrum of a one-cm InGaAsP/InP laser bar operated cw. The spectrum was taken at a current of 80 A. The microchannel heatsink coolant temperature was 11 $^{\circ}$ C and the flow rate and pressure were \sim 2 cm³/min and 50 psi, respectively.

One package from this lot of bars was lifetested. Initially the bar was “burned in” under constant current (115 A) using pulsed conditions (50 μ s). The laser bar produced 20 W and experienced no discernable degradation after 1.2×10^6 shots. Afterwards, the same laser bar was operated at 8W cw, which is near the peak wall plug efficiency for the device. The microchannel heatsink coolant temperature was 11 $^{\circ}$ C and the flow rate and pressure were \sim 2 cm³/min and 50 psi, respectively. A linear degradation rate of 0.17 W/khr was fitted over 7000 hours of lifetesting. This data suggests a 10,000 lifetime with a 20% degradation in output power.

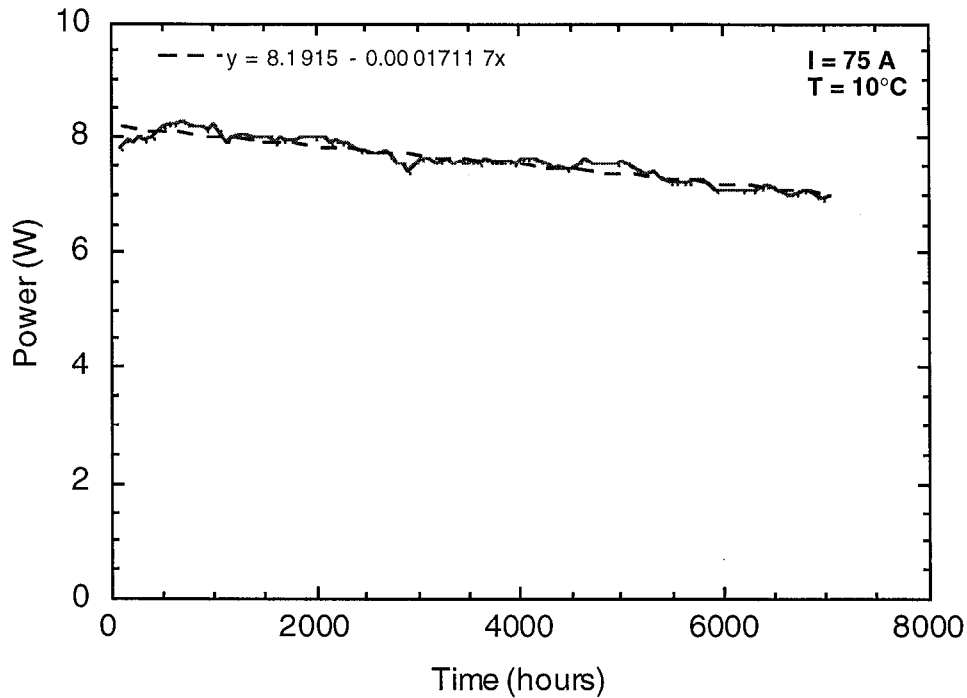


Fig.5. Constant-current lifetest data for a 1.73 μm laser bar operated at 8 W cw. The degradation extrapolates to a 20% power loss for 10,000 hours of operation.

III. LASER DIODE ARRAY

Before packaging into a laser diode arrays, ten unscreened packages were characterized. The slope efficiency of the devices were $0.30 \pm .014 \text{ W/A}$ for the ten packages. The small standard deviation given indicates the good uniformity of device characteristics. The laser bars were subsequently radiance-conditioned with aspheric microlenses that were AR-coated at 1.73 μm. Individual diode packages were actively aligned and the collimated fast-axis divergence was measured to be $11 \pm 3.7 \text{ mrad FWHM}$ for the devices. The slow axis divergence was approximately 160 mrad and was not radiance conditioned. These laser bars were then stacked into a linear array with an emitting aperture of one square cm. As shown in Fig. 6a, the laser array was operated up to 120 A and produced more than 200 W of pulsed power (50 μs pulse widths) which was supply limited. The soft turn-on behavior indicates the variation in threshold current among the devices. In the linear part of the data, the slope is 2.63 Watt/Amp, which extrapolates to a 33 A threshold current. Also shown is the wall plug efficiency for the diode array which is approximately 15% of the array design point of 200 W. As discussed previously, this design point of 200 W (20W/bar) was chosen for highly reliably diode operation. The short pulse width (50 μs) is more than adequate for saturating the upper level of $\text{Cr}^{2+}:\text{ZnSe}$, which has a lifetime of only 9 μs.

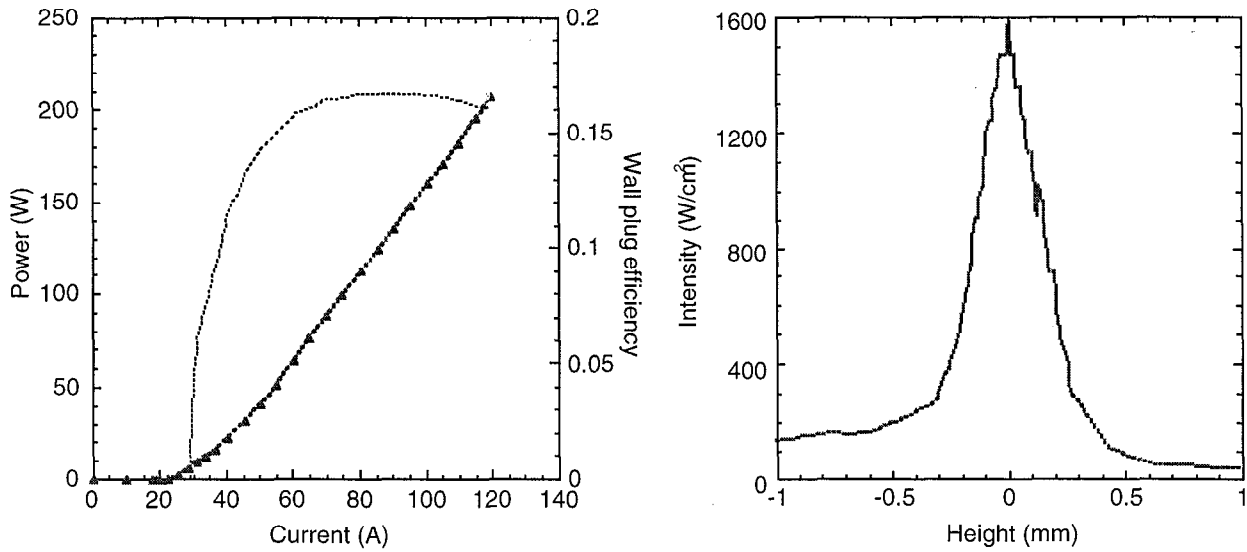


Fig.6. (a) Light-current characteristics for a two-dimensional microlensed array composed of ten packages with a square cm aperture. The device was tested pulsed with 50 μ s pulse widths at 15 $^{\circ}$ C coolant temperature. **(b)** Intensity vs position of the focused diode emission at the beam waist. The peak intensity is 1.6 kW/cm².

The output emission from the array was focused by a 12.7 mm-focal-length cylindrical lens. As shown in Fig 6b, a FWHM spot width of $\sim 300 \mu$ m was achieved. Due to some misalignment of the various packages, the central spot contained 60% of the output power. At the focal region, the peak intensity ranged up to 1.6 kW/cm², an appreciable value with respect to saturation intensities of intra-ion transitions in dielectric hosts. Such a high brightness makes the low-divergence diode-bar array suitable for pumping dopant:host IR laser systems.

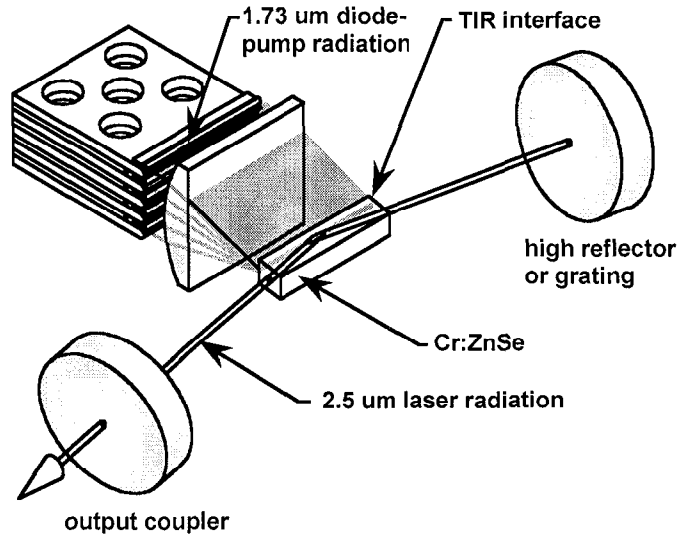


Fig.7. Schematic diagram of Cr:ZnSe DPSSL which utilizes a side-pumped architecture and a 10-bar microlensed laser diode array.

A Cr:ZnSe DPSSL was fabricated and utilized a side-pumped architecture as shown in Fig. 7. The design is based on that of a previously-reported diode-pumped Nd:YVO₄ laser.[13] The output of the diodes is focused with a cylindrical lens (see Fig. 6b) onto a ZnSe slab, whose end faces are AR-coated for 2.5 μm operation. The single bounce at the “TIR interface” allows the resonated beam to sample the high-gain pump face region, and still enter and exit the crystal without aperture losses. Output energy and beam quality depend on bounce angle and penetration of the pump light. Using higher power diodes operating near the peak crystal absorption, we were able to increase the maximum output power of the laser over previous reports.[14]

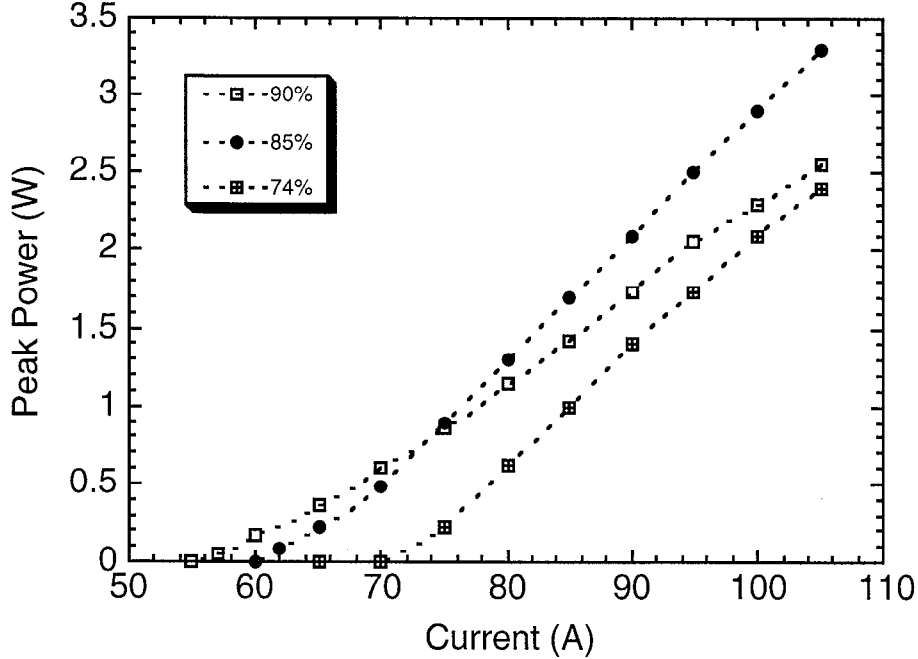


Fig.8. Slope data for the diode-pumped Cr:ZnSe laser operating with several different flat output couplers. The device was tested pulsed with 50 μs pulse widths and produced over 3W of peak power.

A confocal cavity with a 10-cm radii mirror was used in a side pumped configuration in order to aid alignment. As shown in Fig. 8., the 85% output coupler is the optimum choice at this pump level (2 to 3 times threshold). With an input diode power of 200W at 50 μs pulse width, the Cr:ZnSe laser produced over 3 W of peak power at an emission wavelength of 2.5 μm (the peak of the gain curve).

IV. CONCLUSION

We have fabricated high-power, long-wavelength InGaAsP/InP diode bars. The diodes are reliable under pulsed or cw conditions. Under cw operation, the diodes extrapolate to 10,000 hours of operation with 20% degradation in power level. The diode bars were microlensed and integrated into a linear stack that produced over 200 W of pulsed power at an emission wavelength of 1.73 μm . At these operating conditions, over 3 W of pulsed power was produced in a Cr:ZnSe DPSSL at lasing wavelength of 2.5 μm . This illustrates the potential for building compact widely-tunable DPSSLs with high reliability.

ACKNOWLEDGEMENTS

The authors are thankful for the technical expertise of Joe Satariano, Ray Beach, Nils Carlson and the support of Steve Payne, William Krupke, and Howard Powell. This work was performed under the auspices of the U. S. Department of Energy by Lawrence Livermore National Laboratory under contract W-7405-Eng-48.

REFERENCES

- [1] T. Y. Fan, G. Huber, R. L. Byer, and P. Mitzscherlich, "Spectroscopy and Diode Laser-Pumped Operation of Tm, Ho: YAG," *IEEE J. Quantum. Electron.* vol. 24, p. 924-933, 1988.
- [2] R. M. Percival, D. Szebesta, C. P. Seltzer, S. D. Perrin, S. T. Davey, and M. Louka, "A 1.6- μm Pumped 1.9- μm Thulium-Doped Fluoride Fiber Laser and Amplifier of Very High Efficiency," *IEEE J. Quantum. Electron.* vol. 31, p. 489-493, 1995.
- [3] H. Moreira, M. Campos, M. Sawusch, J. M. McDonnell, B. Sand, and P. J. McDonnell, "Holmium Laser Thermokeratoplasty," *Ophthalmology*, vol. 100, p. 752-761, 1993.
- [4] H. K. Choi, G. W. Turner, and S. J. Eglash, "High-Power GaInAsSb-AlGaAsSb Multiple-Quantum-Well Diode Lasers Emitting at 1.9 μm ," *IEEE Photon. Technol. Lett.* vol. 6, p. 7-9, 1994.
- [5] R. H. Page, K. I. Schaffers, L. D. DeLoach, G. D. Wilke, F. D. Patel, J. B. Tassano, Jr., S. A. Payne, W. F. Krupke, K.-T. Chen, and A. Burger, "Cr²⁺-Doped Zinc Chalcogenides as Efficient, Widely Tunable Mid-Infrared Lasers," *IEEE J. Quantum. Electron.* vol. 33, p. 609-619, 1997.
- [6] J. A. Curcio and C. C. Petty, "The Near Infrared Absorption Spectrum of Liquid Water," *J. Opt. Soc. Am.* vol. 41, p. 302-304, 1951.
- [7] M. V. Zolotarev, B. A. Mikhailov, L. I. Alperovich, and S. I. Popov, "Dispersion and absorption of liquid water in the infrared and radio region of the spectrum," *Opt. Spectrosc.* vol. 27, p. 430-432, 1969.
- [8] R. W. H. Engelmann, C-L Shieh, and C. Shu, Chapter 3: "Multiquantum Well Lasers: Threshold Considerations," in *Quantum Well Lasers* edited by P. Zory, p. 72-78, 131-188, 329-352, 1993.
- [9] P. J. A. Thijs, L. F. Tiemeijer, J. J. M. Binsma, and T. van Dongen, "Progress in Long-Wavelength Strained-Layer InGaAs(P) Quantum-Well Semiconductor Lasers and Amplifiers," *IEEE J. Quantum Electron.* vol. 30, p. 477-499, 1994.
- [10] R. J. Beach, W. J. Bennett, B. L. Freitas, D. Munding, B. J. Comaskey, R. W. Solarz, and M. A. Emanuel, "Modular Microchannel Cooled Heatsinks for High Average Power Laser Diode Arrays," *IEEE J. Quantum Electron.* vol. 28, p. 966-976, 1992. The thermal impedance < 0.015 °C-cm²/W was measured at the footprint of a 330 μm cavity length diode bar supplied by Siemens.
- [11] Grown by Epitaxial Products International (Cardiff, U.K).
- [12] J. A. Skidmore, B. L. Freitas, C. E. Reinhardt, E. J. Utterback, R. H. Page, and M. A. Emanuel, "High-Power Operation of InGaAsP-InP Laser Diode Array at 1.73 μm ," *IEEE Photon. Technol. Lett.* vol. 9, p. 1334-1336, 1997.
- [13] J. E. Bernard and A. J. Alcock, "High-efficiency diode pumped Nd:YVO₄ slab laser," *Opt. Lett.* vol. 18, p. 968-970, 1993.
- [14] R. H. Page, J. A. Skidmore, K. I. Schaffers, R. Beach, S. A. Payne, and W. F. Krupke, "Demonstrations of diode-pumped and grating-tuned ZnSe:Cr²⁺ lasers," *Proceedings of Advanced Solid-State Lasers '97*, Orlando, FL (January, 1997).